Surface-enhanced second-harmonic diffraction: Experimental investigation of selective enhancement

Andrew C. R. Pipino,* Richard P. Van Duyne, and George C. Schatz

Department of Chemistry, Northwestern University, 2145 Sheridan Road, Evanston, Illinois 60208-3113

(Received 24 July 1995; revised manuscript received 23 October 1995)

Recent theoretical predictions demonstrating large enhancements of second-harmonic diffraction through the control of surface harmonic composition when the surface-plasmon polariton (SPP) is excited on a corrugated silver surface have been investigated experimentally for the specular order. Interpretation of the mechanism of enhancement in terms of a three-step selective scattering process involving only two spatial harmonics has been found to be justified. Fourier blaze holography, which permits the phase- and amplitude-controlled superposition of multiple harmonics in photoresist, has been used to fabricate the nanostructured, biperiodic gratings. Surfaces have been characterized by atomic force microscopy and Heitmann's method. As predicted, surfaces with optimized spatial frequency composition equal or exceed randomly rough surfaces in the enhancement of second-harmonic reflection relative to a flat silver surface. Enhancement produced by simultaneous excitation of counterpropagating SPP modes at the pump and second-harmonic frequencies has also been detected by varying grating wave vector to tune through a double resonance condition. Factors affecting the quantitative agreement between enhancement measurements and theoretical predictions are briefly discussed.

I. INTRODUCTION

Since the first observation of the effect of Chen, de Castro, and Shen,[1] surface-enhanced second-harmonic generation (SESHG) has been an active area of investigation. Although similar to other surface-enhancement phenomena[2] in that excitation of the surface-plasmon polariton (SPP) is largely responsible for the enhancement, the coherent nature of SHG imparts some unique qualities to the effect.

SESHG from a metal-air interface has been produced by diffractive SPP coupling on randomly rough metal surfaces and gratings. Coherent directional SESHG including enhanced normal and backscattering from randomly rough surfaces has recently been investigated in connection with the weak localization of light.[3,4] In the case of SESHG from gratings, we recently examined[5] the effect of coherence and spatial harmonic composition on SPP-enhanced second-harmonic diffraction from corrugated silver surfaces using the theory of Farias and Maradudin.[6] In the weak corrugation regime where SPP coupling efficiency optimizes, it was shown that scattering of the coherently generated, SPP-enhanced, evanescent second-harmonic wave by spatial harmonics in the surface roughness largely determines the enhancing properties of a particular surface. Enhancement of a specific order could be simply interpreted in terms of a three-step mechanism involving efficient SPP excitation at the pump frequency, generation of a phase-matched evanescent second-harmonic wave, and selective scattering of the evanescent wave into the particular radiative channel. These results suggested that the SHG intensity in a particular order could be maximized on a two Fourier component surface by a mechanism that is distinct from the classical blazing effect. An exception to the three-step mechanism, which involves excitation of counterpropagating SPP modes at the pump and probe frequencies, was also explored. The large magnitude of the enhancements ($\sim 10^4$) predicted for second-harmonic

reflection on optimized surfaces relative to experimentally obtained values on randomly rough surfaces[1,7] further suggested that excitation of the *extended* SPP mode could fully account for the total enhancement.

In this paper, we investigate experimentally the selective enhancement effect for second-harmonic reflection and briefly examine the influence of double resonance. Corrugated surfaces with varied spatial harmonic composition have been fabricated by using the holographic technique, termed Fourier blaze holography, which was originally developed by Breidne *et al.*[8] This technique allows the construction of, in principle, any asymmetric surface profile by superimposing multiple, harmonically related sinusoids with controlled amplitude and phase in photoresist. The surface features produced by the Fourier blaze technique, which are required to be on the order of 10–100 nm in amplitude to optimize SPP coupling effects, have been probed by atomic force microscopy (AFM) and Heitmann's method.[9] To examine the selective enhancement of the second-harmonic specular order, the magnitude of the second spatial harmonic has been varied, since this harmonic directly couples the specular order with the SPP-enhanced, evanescent second-harmonic wave.[5] Our objective is to demonstrate qualitative trends in the surface nanostructure dependence of enhancement. However, factors affecting the quantitative agreement between theory and experiment will be briefly examined with the intent of assessing the influence of very small-scale random roughness on enhancement magnitude.

II. THEORY

Although a theoretical analysis of selective enhancement has been published previously,[5] some additional calculations are presented here to demonstrate previously unexplored aspects of the problem and to provide a coherent presentation. We have used the reduced Rayleigh equations, which were first applied to second-harmonic diffraction, incorporating

     <u>53</u>   4162

the source terms of Sipe *et al.*,[10] by Farias and Maradudin.[6] The theory assumes a p-polarized plane wave is incident from vacuum on a corrugated metal surface, which is described by the general profile function $z = \zeta(x)$. The source terms involve phenomenological parameters,[11] a_s and b_s, for which we use $+0.9$ and -1, respectively, where the a_s value has been measured for silver at 1060 nm.[12] The dielectric response of the metal is described by bulk dielectric constants $\varepsilon(\omega)$ and $\varepsilon(2\omega)$. Unless otherwise specified, we use the values of Dujardin and Theye[13] to demonstrate trends, since these values have shown quantitative agreement with second-harmonic diffraction experiments.[14] The convergence properties of the reduced Rayleigh equations have been discussed elsewhere.[15] Note that enhancements are defined relative to the flat surface efficiency at the same angle of incidence.

III. EXPERIMENT

A. Grating fabrication

Since the original work of Schmahl,[16] the development of holographic methods for the fabrication of grating structures with tailored surface profiles by Fourier synthesis has been an active area of investigation.[8,17,18] The technique of Breidne *et al.*[8] allowed the controlled superposition of spatial harmonics by using the moiré pattern generated by an in-plane reference grating to provide a sensitive probe of the phase relationship between multiple, harmonically related interferometric exposures. A single-mode-stabilized, 457.9-nm laser beam from an argon-ion laser was split, expanded, spatially filtered, and collimated to form two 3-in-diameter beams which were interfered at the film plane. Two flat mirrors, which directed the collimated beams to the film plane, were mounted on 0.01°-resolution rotation stages. The substrates (3×3 in.^{2}) were formed by spin coating 1.5 μm of Shipley 1350B photoresist onto glass plates, which were coated with an iron oxide layer to increase resist-substrate adhesion. The central 2×2 in.^{2} region of the plate was initially covered with an opaque developer-tight mask to allow exposure and development of a reference grating on the perimeter of the active area. A reference fringe density of $1/d = 600$ lines/mm was used, as determined by the angle of intersection between the beams according to the usual relation, $2d\sin\theta = \lambda$, for a symmetrical beam configuration. In practice, because the direct application of this equation to obtain a desired fringe density would require extremely high angular accuracy and precision, the initial plane mirror positions were found by using the moiré pattern generated by a 600-groove/mm *ruled* reference grating. The ruled grating was then replaced with the photoresist plate and a relatively long exposure was used to create a high diffraction efficiency, 600-groove/mm in-plane reference. After development of the reference grating, the photoresist plate and plane mirrors were approximately configured to provide a 1200-line/mm fringe density, which was the desired fundamental spatial frequency. Use of the ruled reference grating assured the accuracy of the groove frequency for subsequent exposures to within a few grooves/mm. As the fringe density approached exactly 1200 lines/mm, large moiré fringes appeared, with the greatest contrast provided by the superposition of diffraction orders that propagated normally to the film

plane. By fine adjustment of the rotation angle of the plane mirrors, the moiré pattern was reduced to one or two fringes to eliminate the phase difference between the fringe density and the reference grating to within approximately a tenth of the period. The mask was then removed to allow exposure of the grating fundamental. A fringe locker,[19] consisting of a pair of photodiodes that provided an error signal to a piezoelectric mirror in the optical system, detected and stabilized the residual moiré pattern thereby fixing the phase of the interference fringes relative to the reference grating. After exposure of the fundamental, the resist plate was reconfigured to permit exposure of the second spatial harmonic at 2400 lines/mm. The moiré pattern was again used to establish the correct fringe density and provide system stabilization. After the third exposure, the entire plate was developed in 6:1-diluted A303 developer. The resulting gratings were then coated with 500 nm of high-purity silver by vacuum deposition at a rate of approximately 1.3 nm/s and stored in a desiccator.

Since the response of the photoresist is nonlinear, a sinusoidal interference pattern will not in general produce a pure sinusoidal grating structure, even for very shallow modulations. Although this nonlinearity can be used to generate a series of profiles with a variable second spatial harmonic amplitude,[20–22] the second-harmonic amplitudes that were predicted to yield the greatest SHG enhancement were too large, relative to the fundamental amplitude, for this approach to be useful. To fully utilize the Fourier synthetic capabilities of the Fourier blaze technique, which allows the independent variation of harmonic amplitudes, the individual exposures must produce nearly pure sinusoidal modulations in the photoresist. As Rosengart and Pockgrand[22] and Raether[23] noted, the fabrication of nearly pure sinusoidal gratings requires the use of a uniform pre-exposure, which permits the most linear region of the exposure versus etch depth curve to be used for the interferometric exposure thereby minimizing, but not completely eliminating, the presence of higher harmonics. To assure that the superimposed exposures contributed nearly pure, sinusoidal components to the surface profile, an optimal uniform pre-exposure was first determined and then used for all subsequent fabrications. Interferometric exposure times for each harmonic were selected by developing a calibration surface, at constant laser power density, which determined groove depth versus exposure and development conditions. The amplitudes of surface features were probed quantitatively by diffraction measurements with s-polarized light (Heitmann's method) at 632.8 nm, which were relatively insensitive to variations in the metal dielectric function. AFM was also used as a probe of surface structure, but Heitmann's method permitted a more convenient average over the surface structure, which varied in amplitude by as much as 25% over the relevant 2×2 in.^{2} region. The resulting grating profiles were well described by the function

$$\zeta(x) = A\left\{\sin\frac{2\pi x}{a} + B\sin\frac{4\pi x}{a}\right\}, \tag{1}$$

where A is a small fraction of the period, B is expressed as a fraction of A, and $\mathbf{a} = 833.3$ nm is the period. Figure 1 shows AFM traces for a series of photoresist profiles for which B
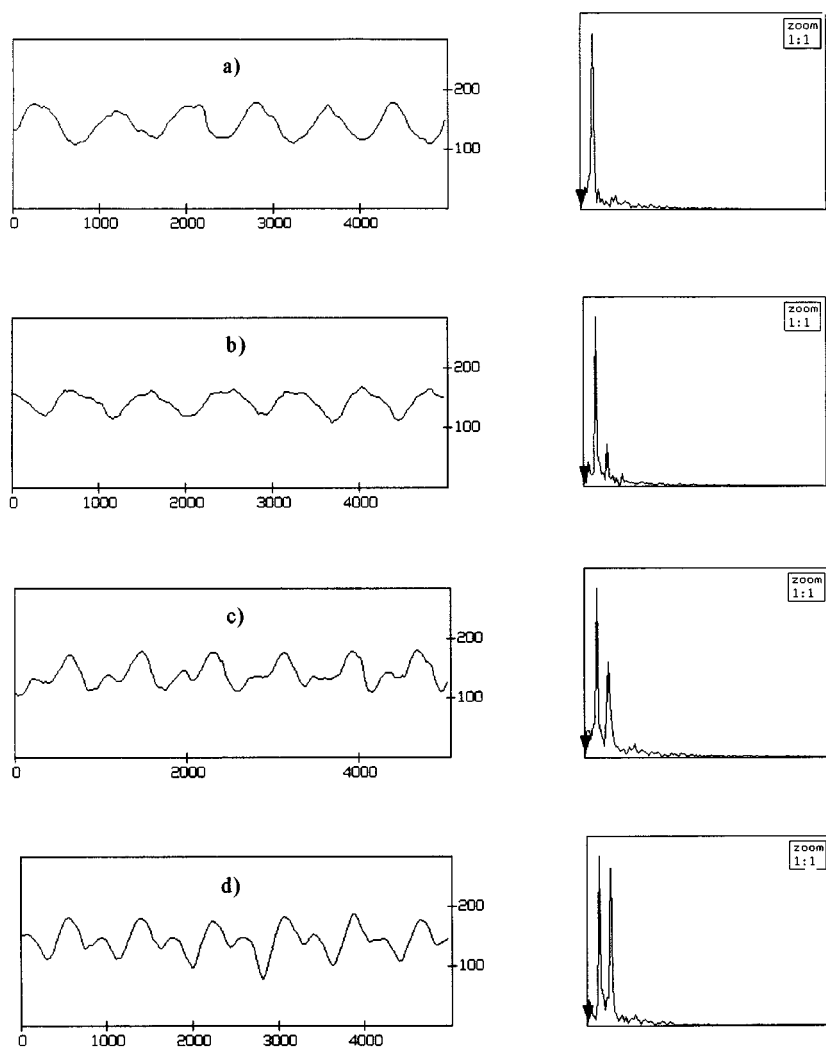
FIG. 1. Atomic force microscopy (AFM) line scans of a series of photoresist profiles produced by the Fourier blaze technique. The Fourier transforms of the profile scans are shown on the right. The first harmonic for all four profiles was exposed simultaneously, followed by a variable second spatial harmonic. Expressed as a fraction of the fundamental amplitude, the second-harmonic amplitudes are approximately: (a) ∼3%, (b) ∼20%, (c) ∼50%, (d) ∼90%. Note that (a) is a nearly pure sinusoidal and that (b)–(d) are well described as a superposition of two Fourier components. Units are in nanometers.

ranges approximately as $0 \leq B \leq 1$, along with the corresponding Fourier transforms. The series was obtained by first exposing the entire central 2×2 in.[2] area with the first harmonic, followed by separate second-harmonic exposures over approximately 1×1 in.[2] areas with the remainder of the active area masked off. This allowed controlled variation of the efficiency of scattering of the SPP-enhanced, second-harmonic evanescent wave with fixed SPP coupling efficiency at the pump frequency. As shown in Fig. 1, nearly pure two Fourier component surfaces are indeed obtained.

B. Second-harmonic-generation measurements

A schematic diagram showing the system used for the 0.013° angle-resolved SHG measurements is shown in Fig. 2. The Q-switched, 1064-nm output of a pulsed yttrium-aluminum-garnet laser operating at 10 Hz was propagated to the far field following a 3:1 beam diameter reduction.[24] After filtering the 532-nm radiation (Schott RG670) arising from Pellin-Broca and beam steering prisms, the unfocused 2-mm-diameter, 2–4-mJ/pulse beam was incident on a silver grating. By mounting the grating and a silvered mirror on opposite legs of a 90° reflector, which was centered on a high-resolution rotation stage, the incident and reflected beams were always in parallel propagation. The angle of incidence could then be varied while the collection optics remained

fixed. This strategy also allowed the flat silver surface SHG, required for calculating enhancement, to be easily measured under identical alignment conditions. By tuning off the SPP resonance, the grating served as a mirror that directed the majority of the incident power to the silvered mirror at the complementary angle of incidence. At this angle, the flat surface SHG was measured with a high signal-to-noise ratio. This result was then used to obtain the flat surface signal at the actual angle of incidence by scaling in accordance with theory in the zero corrugation limit, after a small correction for the reflectivity of the grating. After blocking the 1064-nm pump beam with dichroic mirrors and Schott glass filters (KG5 and/or KG3), the grating-enhanced and flat surface SHG were dispersed by a monochromator and detected by a 1P28 photomultiplier tube (PMT). A reference channel was formed by directing a split-off fraction of the incident pump beam through a quartz disk followed by several KG5 filters, a monochromator, and a 1P28 PMT. The outputs of the sample and reference PMT's were amplified ×10 (Lecroy VV101B) and collected by a dual-channel boxcar averager (PAR-model 162 and two model 165's), which used a 50-ns aperture duration and was triggered by a reversed-biased photodiode. Since exponential averaging was used, the angular velocity of the motorized, high-resolution rotation stage (Newport model 470 rotation stage and model 855C control-
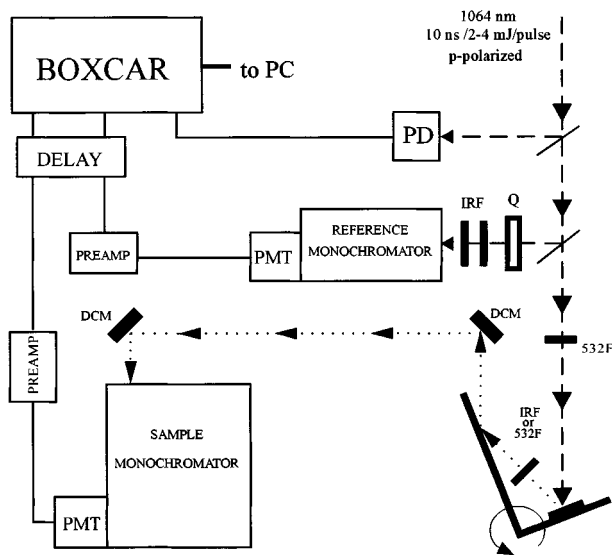
FIG. 2. The optical system used for high-resolution, angle-resolved second-harmonic-generation measurements is shown. The 90° reflector maintains the incident pump and second-harmonic reflected beams parallel over the relevant range of angles of incidence thereby allowing the collection optics to remain fixed. The flat silver surface SHG at the complement to the angle of incidence is obtained by changing filters only. This measurement, obtained with high signal-to-noise ratio, is compared with theory to estimate the flat surface response at the actual angle of incidence. (DCM =dichroic mirror, IRF=infrared filter, Q=quartz disk, PD =photodiode).

ler) was chosen to maintain the signal at 99% of its steady-state value or better during an acquisition. The scan-to-scan repeatability was ±20% for weakly coupling surfaces, while the more strongly coupling surfaces typically showed ±5% repeatability. Laser damage was observed to occur only on resonance for those surfaces that were efficient SPP couplers at the pump frequency and typically only for pulse energies >4 mJ/pulse. The occasional occurrence of damage did not alter conclusions regarding morphology-dependent trends. The repeatability of enhancement determinations for a series of gratings was typically ±10% for strongly coupling surfaces. This was more than sufficient to reveal trends, which in many cases involved changes in SHG efficiency of several orders of magnitude. The accuracy of angular position measurements was estimated to be at best ±0.5°, although a repeatability of ±0.2°, was sufficient to detect some morphology-induced resonance position shifts.

IV. RESULTS AND DISCUSSION

A. Selective enhancement effect

Since the two spatial harmonics required to selectively enhance second-harmonic reflection serve to optimize approximately uncoupled processes, the optimum amplitude for the fundamental harmonic that allows first-order SPP coupling at the pump frequency is expected to correspond approximately to the amplitude that maximizes surface field enhancement on a pure sinusoidal grating [~1.6% (Ref. 5)], as explored previously in connection with surface-enhanced Raman scattering.[25,26] Identifying the optimum amplitude of
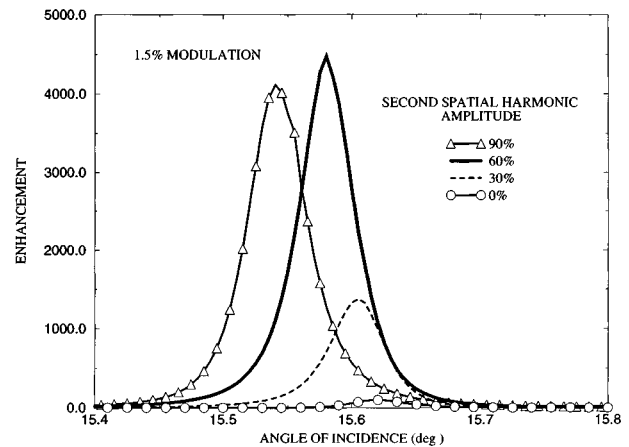
FIG. 3. Calculated second-harmonic reflection enhancement is shown as a function of angle of incidence for a series of surface profiles with a 1.5% modulation. The second spatial harmonic amplitude, expressed as a percentage of the fundamental amplitude, is varied within the series. Note that the higher harmonic significantly enhances second-harmonic reflection and that an optimum value of the amplitude exists.

the second spatial harmonic, which scatters the SPP-enhanced, evanescent wave into the specular order, is less obvious. Intuitively, an optimum amplitude should exist, although it may result from loss of coupling efficiency at the pump frequency as the amplitude is increased. Figure 3 shows the results of calculations demonstrating the dependence of enhancement magnitude on the second spatial harmonic amplitude for a series of odd-symmetry, theoretical profiles with different values of the second spatial harmonic amplitude. Similar but symmetric profiles were considered in Ref. 5. A rapid increase in second-harmonic reflection is observed initially as the higher harmonic amplitude is increased, along with a small shift of the optimum coupling angle to shallower incidence. Note that there is at least a two-order-of-magnitude increase in the enhancement between the pure sinusoidal case and the most strongly enhancing biperiodic profile. An optimum value for the second spatial harmonic amplitude is also found. The full width at half maximum (FWHM) for these peaks is seen to remain approximately constant as a function of second spatial harmonic amplitude, with this value being largely determined by the fundamental amplitude. This is consistent with an interpretation of the selective enhancement effect in terms of a three-step mechanism in which the two diffractive scattering steps involve separate spatial harmonics that make approximately independent contributions. The relative phase of the two spatial harmonics is also important, as depicted in Fig. 4, where the dependence of enhancement on phase shift, expressed as a fraction of the period, is shown for fixed values of the modulation and second-harmonic amplitude. The range of variation of the enhancement is approximately 50%, with an optimum value of the phase occurring at 0.5**a**. Note that, according to the calculations of Fig. 4, for a series of Fourier blaze gratings in which the second spatial harmonic amplitude is varied at fixed modulation, an error in the phase between harmonics of 0.1**a** will not significantly influence detection of the trends predicted in Fig. 3.
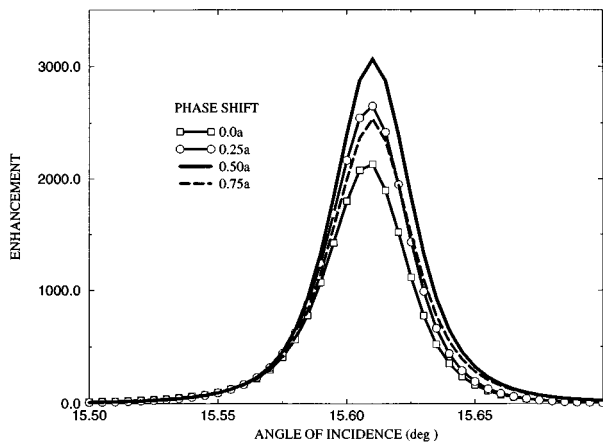
FIG. 4. The calculated effect of the phase shift between the fundamental and second spatial harmonic on enhancement of second-harmonic reflection is shown. The existence of an optimum value of the relative phase is predicted.

Figures 5(a) and 5(b) show measurements of second-harmonic reflection as a function of angle of incidence, which probe the effect predicted in Fig. 3, for two series of profiles. The two series, which were fabricated by the Fou-
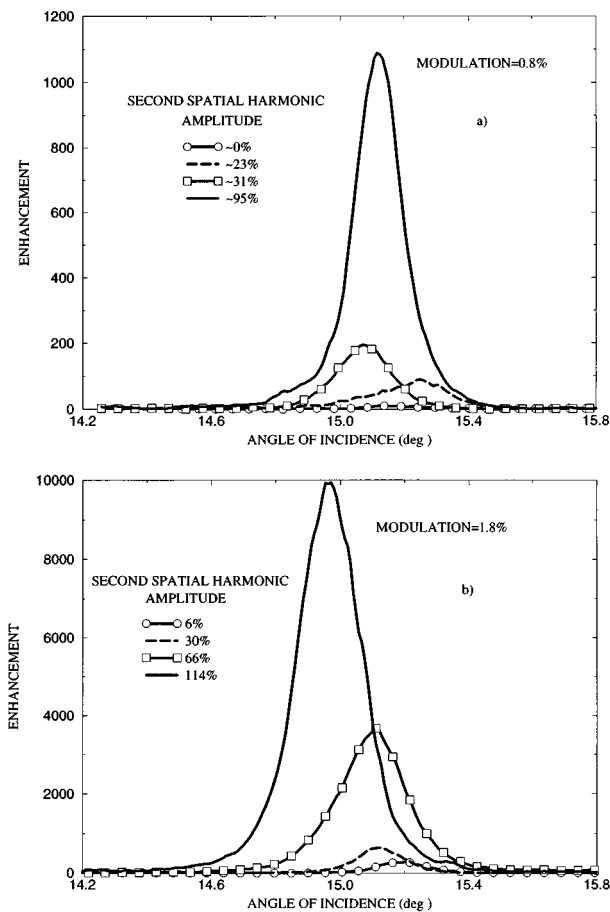
FIG. 5. Measurements demonstrating the selective enhancement effect are shown for two modulations: (a) 0.8% and (b) 1.8%. A large increase in efficiency is observed as the second spatial harmonic amplitude is increased. Also note the nearly constant FWHM for each series.

rier blaze technique, differ in modulation. The second spatial harmonic amplitudes, as measured by Heitmann's method, are similarly expressed as a percent of the fundamental amplitude. The major trend predicted in Fig. 3 of a rapid increase in second-harmonic reflection with increasing second spatial harmonic amplitude is observed. The FWHM as a function of second-harmonic amplitude is also found to remain approximately constant as predicted, although a substantial difference in peak width between theory and experiment is found. This likely results from a significant difference in dielectric function for the real versus calculated systems, as discussed below. With respect to enhancement magnitudes, the nearly pure sinusoidal gratings in each series show substantially different enhancements. This likely arises from the combination of a more efficiently excited SPP-enhanced, evanescent second-harmonic wave and a larger residual second spatial harmonic for the deeper modulation case. The 1.8% modulation series also shows approximately an order-of-magnitude greater enhancement relative to the 0.8% modulation case for the largest value of the second spatial harmonic. Since there was a practical limitation on the number of second-harmonic exposures that we could obtain for a given fundamental exposure, the range of second-harmonic amplitudes within a given series was limited. Although this range was insufficient to observe an optimum in either case, it is probable that the strongest enhancing surface in Fig. 5(b) is nearly optimized. Based on theoretical predictions not shown, a larger-amplitude second spatial harmonic would be required to achieve maximum enhancement for the shallower modulation of Fig. 5(a).

B. Double resonance condition

In addition to exploring the selective enhancement effect, the influence of SPP coupling at the second-harmonic frequency was also probed. As a result of greater dielectric losses at 532 nm, enhancement due to single resonance SPP coupling at the second-harmonic frequency can be expected to be smaller than for coupling at the pump wavelength. However, for certain values of the surface corrugation wave vector, determined simply by the simultaneous solution of the diffractive coupling equations, the SPP at both pump and probe frequencies can be excited in first order. Enhancements as large as 10^4 are predicted for a sinusoidal surface that satisfies this condition.[5] Figure 6 shows calculations of this effect for a series of 3% modulation, pure-sinusoidal profiles, where the angular region scanned for each grating corresponds to first-order SPP coupling at the pump wavelength. The enhancement resulting from double resonance is pronounced. The effect is also seen to be highly localized as a function of wave vector. The inset in Fig. 6 provides a diagrammatic interpretation in terms of first-order coupling to counterpropagating SPP modes at the pump and signal frequencies.

To search for the double resonance experimentally, a series of nearly pure sinusoidal profiles were fabricated with different periods, but with an approximately constant modulation. Figure 7 shows the experimental results obtained, where the modulation of these profiles was approximately 2%. The variation in FWHM of the peaks is indicative of a variation in modulation that arises from the limited control of the fabrication process. As the grating period is decreased,
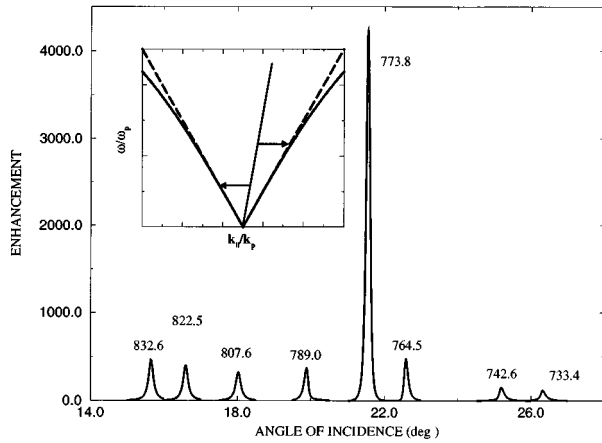
FIG. 6. Calculations of enhancement of second-harmonic reflection for a series of 3% modulation, pure sinusoidal gratings with different periods, as specified in nanometers above each resonance peak. The double resonance effect is predicted to be stronger at this deeper modulation. The inset provides a diagrammatic interpretation of the double resonance condition.

the -1 order coupling angle increases. Since enhancement is defined relative to the flat surface efficiency, which increases rapidly with angle of incidence, the enhancement is expected to decrease rapidly for increasing grating wave vector. This effect is observed for the gratings with periods of 832.6–807.6 nm. Yet in the vicinity of the 773.8-nm period, which satisfies the double coupling condition, enhancement increases to a maximum. A gain of approximately a factor of 5 due to the double resonance is estimated. At higher wave vectors, the trend of decreasing enhancement returns. Although the double resonance effect detected experimentally is not as pronounced as that demonstrated in Fig. 6, this difference likely results from a difference between the actual
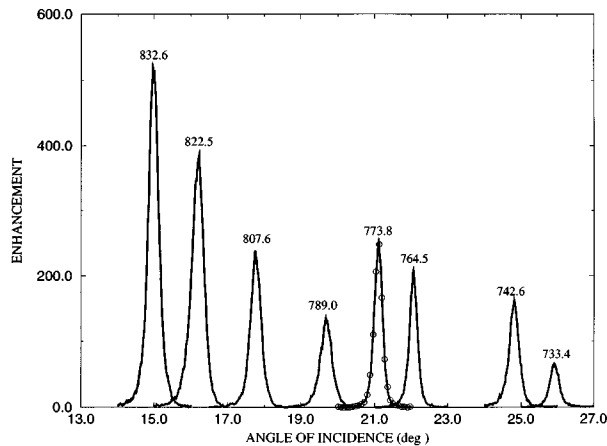
FIG. 7. Measurements demonstrating the influence of SPP coupling at the second-harmonic frequency are shown for a series of nearly pure sinusoidal gratings with an approximately constant modulation of ~2% but different periods. A comparison of the FWHM of the peaks provides an estimate of the variation in modulation. Enhancement typically declines with increasing grating wave vector largely due to the increase in coupling angle. The peak in enhancement for the 773.8-nm grating arises as a result of direct coupling to the SPP modes at both the pump and probe frequencies.

and assumed dielectric functions, as well as the difference in modulation, since the dielectric function affects both the enhancement magnitude and the optimum period for double resonance.

C. Quantitative theory-experiment comparison

Although the objective of this investigation has been to detect trends in the dependence of enhancement on surface nanostructure, the quantitative comparison of theory and experiment will be briefly considered. Previous investigations have shown that by transferring a photoresist profile into a glass or quartz substrate followed by metal deposition, quantitative agreement between theory and experiment for both linear[27,28] and second-harmonic diffraction[14] can be achieved. Measurements involving a metal and transparent-substrate interface have also shown good agreement with respect to line shape.[29] When the grating profile is transferred into a substrate by, for example, ion milling followed by vacuum deposition of metal, the presence of small-scale roughness, which appears to be especially severe for metal deposition directly onto photoresist, is apparently reduced as demonstrated by Knobloch, Duschl, and Knoll.[27] We deem this to be the preferred strategy for grating fabrication, which is likely necessary for obtaining consistent quantitative agreement between theory and experiment. However, directly coated photoresist gratings are sufficient for demonstrating trends in the spatial harmonic composition dependence of SPP enhancement. When disagreement occurs between a rigorous linear diffraction theory and experiment, the discrepancy can typically be attributed to either the dielectric function, which can vary widely with deposition conditions,[13] or inaccurate knowledge of the actual surface profile. In the case of second-harmonic diffraction, the additional factor of the accurate description of the nonlinear susceptibility also becomes important, although for silver at 1060 nm, the source terms of Sipe et al.[10] apparently account for the nonlinear response quantitatively.[14]

Knowledge of the surface profile is especially important for modeling second-harmonic diffraction due to the sensitivity of diffraction orders to selective enhancement.[5,14] A contribution to enhancement from small-scale random roughness can also be anticipated.[30] Depending upon experimental conditions, spheroidal particles can be produced by vacuum deposition that are well known to have plasmon resonances capable of strong angle-of-incidence and polarization-independent surface enhancement for specific frequency ranges.[31] Since enhancement of second-harmonic diffraction due to the comparatively large-scale deterministic roughness of the grating structure is defined relative to the efficiency of a flat surface deposited under the same conditions, these measurements should be less sensitive to resonances arising from small-scale roughness, although the off-resonance raw signal should show random-roughness-induced enhancement.

In Fig. 8, a detailed fit for the specular order enhancement of a shallow, nearly pure sinusoidal silver grating was attempted. Numerical results obtained using the dielectric function data of Ref. 32 (solid curve) provided the best fit to the data (circles) for this particular profile. However, a thorough attempt to fit the data of Fig. 5 with these optical constants failed to account for the peak enhancement of Fig.
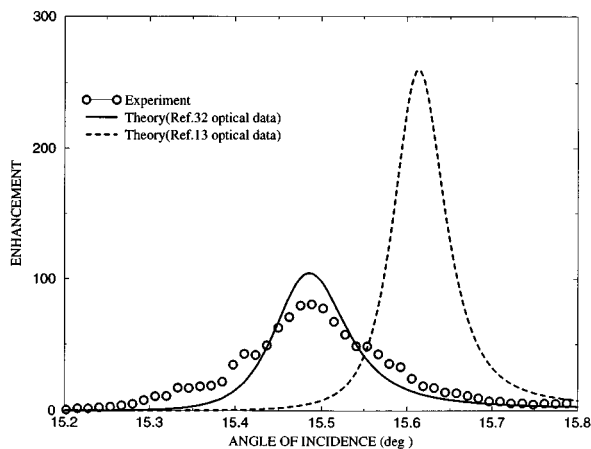
FIG. 8. A quantitative fit of theory to experiment (circles) is attempted for enhancement of second-harmonic reflection from a nearly pure sinusoidal grating with a modulation of 2.0%, as measured by Heitmann's method. The theoretical curves were obtained with dielectric functions from Ref. 32 (solid) and 13 (dashed).

5(b). Larger enhancements can be obtained by using the dielectric data of Ref. 13, as shown by the dashed curve in Fig. 8, although the FWHM fit is then less satisfactory. An additional factor that likely complicates quantitative analysis of our results is the potential for local variation in the groove depth, since the enhancement magnitude is very sensitive to this parameter. However, it is interesting to note that no off-resonance raw SHG signal was detectable, which suggests that at most only a weak enhancement due to small-scale random roughness was present.

V. CONCLUSION

The selective enhancement effect, which results from direct connection of the SPP-enhanced, evanescent second-harmonic wave to a particular diffraction order through a specific spatial harmonic, has been shown to increase the efficiency of second-harmonic reflection from a silver grating by 10^2 relative to a pure sinusoidal grating of the same modulation and by 10^4 relative to a flat silver surface. A coherent source of SHG in reflection has thereby been created. Fourier blaze holography has been successfully used to fabricate the shallow, biperiodic surfaces. The specular second-harmonic order explored here is predicted to be the least sensitive order for selective enhancement.[5] These results demonstrate that the enhancement properties of diffraction gratings can typically be interpreted in terms of a three-step mechanism. An exception to this situation, which arises under conditions of double resonance, has also been detected. Although agreement between theory and experiment has been largely qualitative, we expect that quantitative agreement should be achievable.

In connection with recent investigations of enhanced, directional SHG from randomly rough surfaces,[3,4,34] it is worth noting that the selective enhancement effect could influence the magnitude of these directional enhancements. As explored in the theoretical investigation by McGurn, Leskova, and Agranovich,[3] multiple scattering by a disordered surface of an SPP wave generated at the pump frequency is expected to excite a counterpropagating SPP wave that interferes with the incident SPP. Second-harmonic photons are then generated at the null wave vector through the second-order susceptibility of the surface. The selective enhancement effect may be important since when the minigap region where counterpropagating SPP waves are excited[33] is probed, specific second-harmonic diffraction orders correspond to 0° scattering and backscattering that can be selectively enhanced by appropriate spatial harmonics.

ACKNOWLEDGMENTS

*Present address: Chemical Kinetics and Thermodynamics Division, Chemistry Building Room A260, National Institute of Standards and Technology (NIST), Gaithersburg, MD 20899.

[1] C. K. Chen, A. R. B. de Castro, and Y. R. Shen, Phys. Rev. B 46, 145 (1981).

[2] M. Moskovits, Rev. Mod. Phys. 57, 783 (1985).

[3] A. R. McGurn, T. A. Leskova, and V. M. Agranovich, Phys. Rev. B 44, 11 441 (1991).

[4] O. A. Aktsipetrov, V. N. Golovkina, O. I. Kapusta, T. A. Leskova, and N. N. Novikova, Phys. Lett. A 170, 231 (1992).

[5] A. C. R. Pipino, G. C. Schatz, and R. P. Van Duyne, Phys. Rev. B 49, 8320 (1994).

[6] G. A. Farias and A. A. Maradudin, Phys. Rev. B 30, 3002 (1984).

[7] G. T. Boyd, Th. Rasing, J. R. R. Leitz, and Y. R. Shen, Phys. Rev. B 30, 519 (1984).

[8] M. Breidne, S. Johansson, L.-E. Nilsson, and H. ÅhlÈn, Optica Acta 26, 1427 (1979).

[9] D. Heitmann, Opt. Commun. 20, 292 (1977).

[10] J. E. Sipe, V. C. Y. So, M. Fukui, and G. I. Stegeman, Phys. Rev. B 21, 4389 (1980).

[11] J. Rudnick and E. A. Stern, Phys. Rev. B 4, 4274 (1971).

[12] J. C. Quail and H. J. Simon, Phys. Rev. B 31, 4900 (1985).

[13] M. M. Dujardin and M. L. Theye, J. Phys. Chem. Solids 32, 2033 (1971).

[14] J. C. Quail and H. J. Simon, J. Opt. Soc. Am. 5, 325 (1988).

[15] E. Popov and M. Neviere, J. Opt. Soc. B 11, 1555 (1994).

[16] G. Schmahl, J. Spectrosc. Soc. Jpn. Suppl. 23-1, 3 (1974).

[17] L. Cescato, G. F. Mendes, and Jaime Frejlich, Appl. Opt. 27, 1988 (1988).

[18] M. Lida, K. Hagiwara, and H. Asakura, Appl. Opt. 31, 3015 (1992).

[19] D. R. MacQuigg, Appl. Opt. 16, 291 (1977).

[20] S. Austin and F. T. Stone, Appl. Opt. 15, 1071 (1976).

[21] S. Austin and F. T. Stone, Appl. Opt. 15, 2126 (1976).

[22] E.-H. Rosengart and I. Pockrand, Opt. Lett. 1, 194 (1977).

[23] H. Raether, Opt. Commun. 42, 217 (1982).

[24] A. Siegman, Appl. Opt. **13**, 353 (1974).

[25] N. Garcia, Opt. Commun. **45**, 307 (1983).

[26] F. Toigo, A. Marvin, V. Celli, and N. R. Hill, Phys. Rev. B **15**, 5618 (1977).

[27] H. Knobloch, C. Duschl, and W. Knoll, J. Chem. Phys. **91**, 3810 (1989).

[28] D. J. Nash, N. P. K. Cotter, E. L. Wood, G. W. Bradbury, and J. R. Sambles, J. Mod. Opt. **42**, 243 (1995).

[29] H. J. Simon and Z. Chen, Phys. Rev. B **39**, 3077 (1989).

[30] R. P. Van Duyne, J. C. Hulteen, and D. A. Treichel, J. Chem. Phys. **99**, 2101 (1993).

[31] E. J. Zeman and G. C. Schatz, J. Phys. Chem. **91**, 634 (1987).

[32] *Handbook of Optical Constants*, edited by E. D. Palik (Academic, Orlando, FL, 1985).

[33] G. Blau, J. L. Coutaz, and R. Reinisch, Opt. Lett. **18**, 1352 (1993).

[34] L. Kuang and H. J. Simon, Phys. Lett. A **197**, 257 (1995).